

Fluidity of the system produced in relativistic pp and heavy-ion collisions: Hadron resonance gas model approach

Ronald Scaria¹, Dushmanta Sahu¹, Captain R. Singh¹, Raghunath Sahoo^{1,2,*}, and Jan-e Alam³

¹*Department of Physics, Indian Institute of Technology Indore, Simrol, Indore 453552, India*

²*CERN, CH 1211, Geneva 23, Switzerland and*

³*Variable Energy Cyclotron Centre, 1/AF, Bidhan Nagar, Kolkata, India*

(Dated: January 21, 2022)

We have estimated the dimensionless parameters such as Reynolds number (Re), Knudsen number (Kn) and Mach number (Ma) for a multi-hadron system by using the excluded volume hadron resonance gas (EVHRG) model along with Hagedorn mass spectrum to include higher resonances in the system. The size dependence of these parameters indicate that the system formed in proton+proton collisions may achieve thermal equilibrium making it unsuitable as a benchmark to analyze the properties of the system produced in heavy ion collisions at similar energies. While the magnitude of Kn can be used to study the degree of thermalization, the variations of Re and Ma with temperature (T) and baryonic chemical potential (μ_B) assist to understand the change in the nature of the flow in the system - from laminar to turbulent and from subsonic to supersonic, respectively.

PACS numbers:

I. INTRODUCTION

Relativistic heavy-ion collisions aim to create extreme conditions of temperature (T) and baryonic chemical potential (μ_B) so as to melt the hadrons to produce a deconfined state of quarks and gluons, called Quark-Gluon Plasma (QGP). Although initially it was envisaged that such a state of matter would behave as an ideal gas, the analysis of the results of the nuclear collisions at the Relativistic Heavy-Ion Collider (RHIC) and Large Hadron Collider (LHC) energies reveal that the created matter behaves like strongly interacting liquid with lowest shear viscosity (η) to entropy density (s) ratio. The study of experimental data within the framework of relativistic hydrodynamics shows that the η/s of QGP is close to $1/4\pi$, which is the lowest AdS/CFT bound obtained in Ref. [1], indicating the creation of a “perfect fluid” in relativistic heavy-ion collisions at the RHIC [2–5]. So far, the results from proton+proton (pp) collisions were used as a baseline for establishing QCD medium formation in heavy-ion collisions at RHIC and LHC energies. However, recent observations of strangeness enhancement, collectivity, long-range particle correlations etc. in pp and p+Pb collisions at the LHC energies [6, 7] opened a new domain of studies. These observations advocate for the possibility of thermalization and collectivity in the small system produced in pp collisions. Final state multiplicity dependent event characterization and collision centrality selection even in such collisions emerged out with intense search for QGP-like properties in high-multiplicity pp collisions. Although the formation of QGP-droplets is yet to be established, a detailed characterization of the system formed in pp collisions at the LHC through var-

ious theoretical models and experimental searches using new observables are underway. Combining pp, p+Pb and heavy-ion collisions at the LHC energies, final state event multiplicity has become one of the unique observables to describe the system size and collision energy dependence of various observables. In this direction, one tries to find a threshold in the final state multiplicity [8–11] after which QGP-like properties and the corresponding theoretical models to understand a QCD medium formation, including those to study thermalization and hydrodynamic models could be employed.

The nature of the hydrodynamic flow (laminar or turbulent) can be classified based on the magnitude of the Reynolds number (Re). The Mach number (Ma) helps in determining whether the flow is supersonic or subsonic and the Knudsen number (Kn) can be an indicator of thermalization. Fluid with high value of Re may show turbulent behavior. As $Re \sim \frac{\text{inertial force}}{\text{viscous force}} \sim 1/\eta$, systems with low viscosity are likely to manifest turbulent nature. At RHIC energy for a system size of 5 fm and temperature around $T = 300$ MeV, Re varies between 10–100 for a fluid velocity in the range 0.1–1 (in the unit of $c = 1$) [12]. Kn is the ratio between mean free path of the system and the system size. Therefore, Kn value tending to zero implies a system with a high degree of thermalization. A large value of Kn suggests a system that is far from equilibrium and in such a case, the application of hydrodynamics is not allowed. For Au+Au collision at $\sqrt{s_{NN}} = 200$ GeV, the Knudsen number was estimated from a hydrodynamic model, in which the elliptic flow as a function of centrality suggests the value of $Kn \simeq 0.3$ for central collisions and 0.5 for semi-central collisions [13, 14]. Similarly, Mach number is defined as the ratio of the flow velocity to the speed of sound in the system. For $Ma \ll 1$, the fluid density is almost uniform and consequently suggests incompressible flow. Thus, Mach number can help in

*Corresponding author: Raghunath.Sahoo@cern.ch

characterizing the compressibility of the fluid. These three parameters together define the applicability of hydrodynamics and give information about properties like compressibility and viscosity of the fluid [15]. These observables provide a unique way to observe the deviation of a fluid (system) from that of the *perfect fluid* under the limits: $Kn \ll 1$, $Ma \ll 1$ and $Re \gg 1$.

To understand the thermodynamics of the system produced in the ultra-relativistic collisions, inputs from lattice quantum chromodynamics (LQCD) has been extremely useful. However, it has limitations, such that it can work accurately for zero or low baryochemical potential ($\mu_B/T \rightarrow 0$). In this context models such as Hadron Resonance Gas (HRG) can be useful to analyze data without having restrictions on the value of baryochemical potential. The HRG model has been used successfully to study the thermodynamics of the hadronic phase that appears in the course of evolution of the system produced in ultra-relativistic collisions. In this article, we have used the HRG model with excluded volume effect along with a Hagedorn mass spectrum to study the thermal behavior of the hadronic phase formed in relativistic collisions [16–18]. This article is organized as follows. Detailed descriptions of the formalism and methodology to calculate the thermodynamic properties are given in Sec. II. In Sec. III, we present the results along with a detailed discussion. Finally, we summarize our study in Sec. IV.

II. FORMALISM

A. Hadron Resonance Gas with Excluded Volume

The hadron resonance gas model describes the hadronic phase of the matter by assuming that the system is composed of free hadrons of different species. It treats various hadrons and their resonances as point particles. However, the existence of repulsive interactions among the hadrons has already been known from the nucleon-nucleon scattering experiments. The excluded volume hadron resonance gas (EVHRG) model takes such repulsive interactions into account. It reduces the volume available for the hadrons to move by the volume that they occupy. The EVHRG model estimations for various thermodynamic observables match the LQCD estimations up to $T \sim 140$ MeV. It is also essential to take into account the effect of the Hagedorn mass spectrum, which includes the yet unmeasured higher masses of the hadrons, as they can have a significant contribution to the Equation of State (EoS) near the critical temperature (T_c).

In a Grand Canonical Ensemble (GCE) of ideal HRG (IHRG) formalism, the partition function for the i^{th} particle can be written as [16];

$$\ln Z_i^{id} = \pm \frac{V g_i}{2\pi^2} \int_0^\infty p^2 dp \ln \{1 \pm \exp[-(E_i - \mu_i)/T]\} \quad (1)$$

where g_i and $E_i = \sqrt{p^2 + m_i^2}$ are the degeneracy and energy of the i^{th} hadron, respectively. The corresponding chemical potential is given by,

$$\mu_i = B_i \mu_B + S_i \mu_S + Q_i \mu_Q, \quad (2)$$

where B_i , S_i and Q_i are the baryon number, strangeness and electric charge of the i^{th} hadron. The μ_B , μ_S , μ_Q are the baryon chemical potential, strangeness chemical potential and chemical potential related to the electric charge, respectively. From the partition function one can obtain the pressure P_i , energy density ε_i , number density n_i and entropy density s_i as follows:

$$P_i^{id}(T, \mu_i) = \pm \frac{T g_i}{2\pi^2} \int_0^\infty p^2 dp \ln \{1 \pm \exp[-(E_i - \mu_i)/T]\} \quad (3)$$

$$\varepsilon_i^{id}(T, \mu_i) = \frac{g_i}{2\pi^2} \int_0^\infty \frac{E_i p^2 dp}{\exp[(E_i - \mu_i)/T] \pm 1} \quad (4)$$

$$n_i^{id}(T, \mu_i) = \frac{g_i}{2\pi^2} \int_0^\infty \frac{p^2 dp}{\exp[(E_i - \mu_i)/T] \pm 1} \quad (5)$$

$$s_i^{id}(T, \mu_i) = \pm \frac{g_i}{2\pi^2} \int_0^\infty p^2 dp \left[\ln \{1 \pm \exp[-(E_i - \mu_i)/T]\} \pm \frac{(E_i - \mu_i)/T}{\exp[(E_i - \mu_i)/T] \pm 1} \right] \quad (6)$$

The effect of higher states and resonances is included into IHRG by making use of the following parametrization for the Hagedorn mass spectrum [19];

$$\rho(m) = C \frac{\theta(m - M)}{(m^2 + m_0^2)^a} \exp\left(\frac{m}{T_H}\right), \quad (7)$$

where M is the mass cut-off for selected hadrons and T_H is the Hagedorn temperature chosen as 180 MeV for our analysis. For other parameters, we have chosen $C = 0.05$ GeV^{3/2}, $m_0 = 0.5$ GeV and $a = 5/4$ [17]. The inclusion of Hagedorn states leads us to adopt Boltzmann approximation. Thus, the previously defined thermodynamic properties are modified as;

$$P^H(T, \mu) = \frac{T}{2\pi^2} \int dm \int_0^\infty p^2 dp \exp\left(-\frac{E - \mu}{T}\right) \times \left[\sum_i g_i \delta(m - m_i) + \rho(m) \right] \quad (8)$$

$$\varepsilon^H(T, \mu) = \frac{1}{2\pi^2} \int dm \int_0^\infty p^2 E dp \exp\left(-\frac{E - \mu}{T}\right) \times \left[\sum_i g_i \delta(m - m_i) + \rho(m) \right] \quad (9)$$

$$n^H(T, \mu) = \frac{1}{2\pi^2} \int dm \int_0^\infty p^2 dp \exp\left(-\frac{E-\mu}{T}\right) \times \left[\sum_i g_i \delta(m - m_i) + \rho(m) \right] \quad (10)$$

$$s^H(T, \mu) = \frac{1}{2\pi^2} \int dm \int_0^\infty p^2 dp \exp\left(-\frac{E-\mu}{T}\right) \times \left(1 + \frac{E-\mu}{T}\right) \left[\sum_i g_i \delta(m - m_i) + \rho(m) \right] \quad (11)$$

Repulsive interactions at short distances are introduced into IHRG by using thermodynamically consistent excluded volume approach [18]. This, in essence is a van der Waals correction. The system volume V is now replaced by the available volume V_{av} ,

$$V \rightarrow V_{av} = V - \sum_i v_i N_i, \quad (12)$$

where $v_i = 16\pi r_i^3/3$ is the excluded volume parameter to take care of two overlapping hadrons (also called as eigen volume) [16, 17] and N_i is the number of particles. From here on, we restrict ourselves to the case of equal volume parameter v_i for all hadrons, $v = 16\pi r_h^3/3$. Use of Eq. 12 in grand canonical ensemble changes pressure through an iterative process [16, 17],

$$P^{ev}(T, \mu) = \kappa P^H(T, \mu), \quad (13)$$

where, κ is the excluded volume suppression factor given by,

$$\kappa = \exp\left(-\frac{vP^{ev}}{T}\right). \quad (14)$$

Accordingly, the thermodynamic entities like ε , n and s are modified as follows;

$$\varepsilon^{ev}(T, \mu) = \frac{\kappa \varepsilon^H(T, \mu)}{1 + \kappa v n^H(T, \mu)} \quad (15)$$

$$n^{ev}(T, \mu) = \frac{\kappa n^H(T, \mu)}{1 + \kappa v n^H(T, \mu)} \quad (16)$$

$$s^{ev}(T, \mu) = \frac{\kappa s^H(T, \mu)}{1 + \kappa v n^H(T, \mu)}. \quad (17)$$

B. *Re*, *Kn* and *Ma* Dynamics in Hadron Gas

The transport properties of hadron gas can be investigated by using the Boltzmann Transport Equation

(BTE) which is given as,

$$\frac{\partial f_p}{\partial t} + v_p^i \frac{\partial f_p}{\partial x^i} + F_p^i \frac{\partial f_p}{\partial p^i} = I(f_p), \quad (18)$$

where v_p^i is the velocity of the i th hadron and F_p^i is the external force acting on it. $I(f_p)$ is defined as the collision integral which gives the rate of change of distribution function due to collisions. The thermal equilibrium in a system is achieved and maintained by the collisions among the constituents. Under the relaxation time approximation the collision integral can be written as:

$$I(f_p) = -\frac{(f_p - f_p^0)}{\tau(E_p)}, \quad (19)$$

here $\tau(E_p)$ is the particle dependent relaxation time and f_p^0 is the equilibrium distribution function defined as;

$$f_p^0 = \exp\left(-\frac{E_i - \mu}{T}\right). \quad (20)$$

For a hadron gas at finite chemical potential, the shear viscosity can be obtained by using the following expression [20],

$$\eta = \sum_i \frac{1}{15T} \int \frac{d^3 p}{(2\pi)^3} \frac{p^4}{E_i^2} (\tau_i f_i^0 + \bar{\tau}_i \bar{f}_i^0) \quad (21)$$

where τ_i is the relaxation time of i^{th} hadron and f_i^0 is its corresponding distribution function. The particle dependent average relaxation time is given by,

$$\bar{\tau}_i^{-1} = \sum_j n_j \langle \sigma_{ij} v_{ij} \rangle, \quad (22)$$

where n_j is the number density of j^{th} hadronic species. Furthermore, considering hadrons as hard spheres of equal radius r_h (having constant cross section $\sigma = 4\pi r_h^2$), the thermal average of total cross section times relative velocity i.e. $\langle \sigma v \rangle$ can be calculated as [20–22],

$$\langle \sigma_{ij} v_{ij} \rangle = \sigma \frac{\int d^3 p_i d^3 p_j v_{ij} f_i^0 f_j^0}{\int d^3 p_i d^3 p_j f_i^0 f_j^0}. \quad (23)$$

Now, rewriting the momentum space volume elements in terms of scattering angle θ [20, 23];

$$d^3 p_i d^3 p_j = 8\pi^2 p_i p_j dE_i dE_j d\cos\theta, \quad (24)$$

the numerator in Eq. 23 becomes

$$d^3 p_i d^3 p_j v_{ij} f_i^0 f_j^0 = \sigma \int 8\pi^2 p_i p_j dE_i dE_j d\cos\theta f_i^0 f_j^0 \times \frac{\sqrt{(E_i E_j - p_i p_j \cos\theta)^2 - (m_i m_j)^2}}{E_i E_j - p_i p_j \cos\theta} \quad (25)$$

and the denominator reads as:

$$d^3 p_i d^3 p_j f_i^0 f_j^0 = \int 8\pi^2 p_i p_j dE_i dE_j d\cos\theta f_i^0 f_j^0. \quad (26)$$

Now $\langle\sigma_{ij}v_{ij}\rangle$ takes the following form

$$\langle\sigma_{ij}v_{ij}\rangle = \frac{\sigma \int p_i p_j dE_i dE_j d\cos\theta f_i^0 f_j^0 \times \frac{\sqrt{(E_i E_j - p_i p_j \cos\theta)^2 - (m_i m_j)^2}}{E_i E_j - p_i p_j \cos\theta}}{\int p_i p_j dE_i dE_j d\cos\theta f_i^0 f_j^0} \quad (27)$$

E_i and E_j are integrated in the limit m_i to ∞ and m_j to ∞ , respectively. The limit of integration of $\cos\theta$ runs from -1 to +1. Finally, the relaxation time is calculated using Eqs. 22 and 27.

The use of Boltzmann states cannot rigorously describe massive Hagedorn states. This makes estimation of their contribution to shear viscosity difficult. These states being highly unstable, decay rapidly and it is reasonable to assume that their presence affects the mean free paths of other hadrons in the medium. They also significantly affect the thermodynamics of hadronic matter close to the QCD critical temperature. Hence their contribution cannot be ignored. The contribution from these states to the shear viscosity can be estimated by using the approximation that the mean free path of such resonances is inversely related to their decay widths [24–26]. The decay width of Hagedorn states is obtained by a linear fit to decay widths of all resonances in particle data book. Assuming that these particles have hard-core radius r_h , the excluded volume approximation of shear viscosity contribution of Hagedorn states is given by,

$$\eta_H = \frac{5T^{3/2}}{128\pi^{5/2}n^H(T)} \int m^{5/2} dm \rho(m) K_{\frac{5}{2}}\left(\frac{m}{T}\right). \quad (28)$$

Here $n^H(T)$ is the number density of Hagedorn states in the medium and K_n is the modified Bessel function of the second kind.

The Reynolds number, which varies inversely to shear viscosity can be written as,

$$Re = \frac{D\langle v \rangle T}{\eta/s^{ev}}, \quad (29)$$

where $\langle v \rangle = m^{-1} \sum_{i=1}^m \int \frac{d^3 p}{(2\pi)^3} v_i f_i^0 / \int \frac{d^3 p}{(2\pi)^3} f_i^0$ is the fluid velocity and D is the system size. The Knudsen number is written as,

$$Kn = \lambda/D, \quad (30)$$

where $\lambda = \frac{1}{\sqrt{2}n^{ev}\sigma}$ is the mean free path of the system.

Finally, the Mach number is written as,

$$Ma = \langle v \rangle / c_s, \quad (31)$$

where

$$c_s^2 = \frac{\frac{\partial P}{\partial T} + \frac{\partial P}{\partial \mu_B} \frac{d\mu_B}{dT}}{\frac{\partial \varepsilon}{\partial T} + \frac{\partial \varepsilon}{\partial \mu_B} \frac{d\mu_B}{dT}}, \quad (32)$$

is the speed of sound in the system which reduces to $c_s^2 = (\frac{\partial P}{\partial \varepsilon})$ at vanishing baryon chemical potential. Here,

$$\frac{d\mu_B}{dT} = \frac{s \frac{\partial n}{\partial T} - n \frac{\partial s}{\partial T}}{n \frac{\partial s}{\partial \mu_B} - s \frac{\partial n}{\partial \mu_B}}. \quad (33)$$

With the help of the formulae given above, we now move forward to estimate the dimensionless parameters Re , Kn and Ma .

III. RESULTS AND DISCUSSION

We include all the hadrons and resonances up to a mass of 2.25 GeV listed in the particle data book [27] along with the Hagedorn spectrum. The thermodynamic properties are dependent on the eigen volume of hadrons which have to be chosen appropriately. It is dependent only on the unknown parameter r_h . The hadron-hadron interactions are not repulsive for an r_h value comparable to the charge radii. Hence, it was argued that r_h should be taken according to the hard-core volume known from nucleon-nucleon scattering. The repulsive interactions are mediated by ω mesons and the range of an interaction is inversely proportional to the mass of the mediator. Based upon the above argument, we have chosen a hard-core radius, $r_h = 0.3$ fm, to incorporate the repulsive interaction. Also there is not much deviation in charge radii between baryons and mesons, therefore, uniform hard-core radius ($r_h = 0.3$ fm) is considered for all hadrons [20, 23, 28].

The effect of system size on volume and particle numbers, considered infinite in the thermodynamic limit, can be implemented by providing a lower momentum cut-off to the integral over momentum space [29–31]. The finite-size effect is introduced by using lower limit of momentum $p_{\text{cutoff}}(\text{MeV}) = 197\pi/D(\text{fm})$ [31]. Here $D = 2R$ is characteristic system size, R being system radius. We chose few representative radii, $R = 3, 5, 7$ and

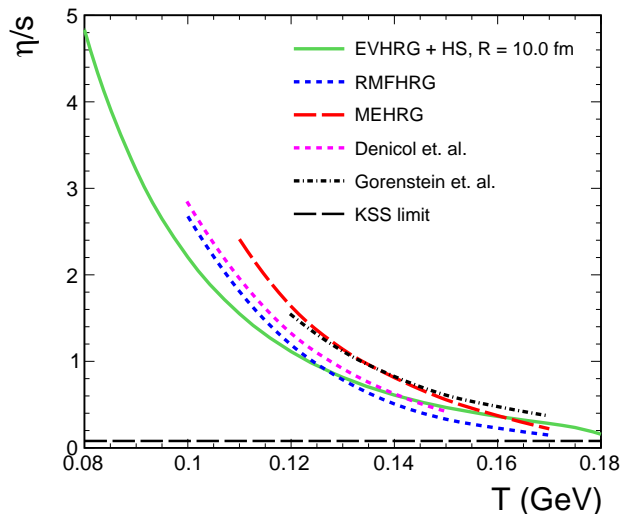


FIG. 1: Comparison of η/s obtained for $R = 10.0$ fm with the estimations of other models at $\mu_B = 0.0$ GeV [24, 35–37].

10 fm to cover system properties from high multiplicity pp to ultra-relativistic heavy-ion collisions [31, 32]. This choice of system size goes inline with the recent observations of finite hadronic phase lifetime observed in pp and heavy-ion collisions [33, 34].

To validate our study, we have compared our results with others in Fig. 1. It shows the dependence of η/s on system temperature for a fixed system size at zero chemical potential ($\mu_B = 0.0$ GeV). The AdS/CFT lower limit to η/s (also known as KSS limit), which is $1/4\pi$ [1], is also shown in the figure. It is observed that the η/s in the given temperature range of the hadronic phase, shows a near perfect fluid behavior towards higher temperature. Our study is in good agreement with the values of η/s obtained by Gorenstein et al., where the authors considered EVHRG within relativistic molecular kinetic theory [35]. We have also compared our η/s values with the results obtained from Chapman-Enskog theory, relativistic mean-field HRG and EVHRG formalism with Hagedorn spectrum [24, 36, 37].

Further, the dependence of the speed of sound on temperature is compared with lattice QCD data at $\mu_B = 0.0$ GeV in Fig. 2. It is observed that c_s^2 obtained in EVHRG formalism is in agreement with the LQCD data except at the high-temperature regime [38], where the HRG model is not a good approximation for the description of the system. The addition of the Hagedorn spectrum accentuates this deviation because of the rapid increase in energy density as compared to pressure on approaching the Hagedorn temperature.

In Fig. 3 the variation of c_s^2 is explored with temperature (T) and chemical potential (μ_B). We have observed

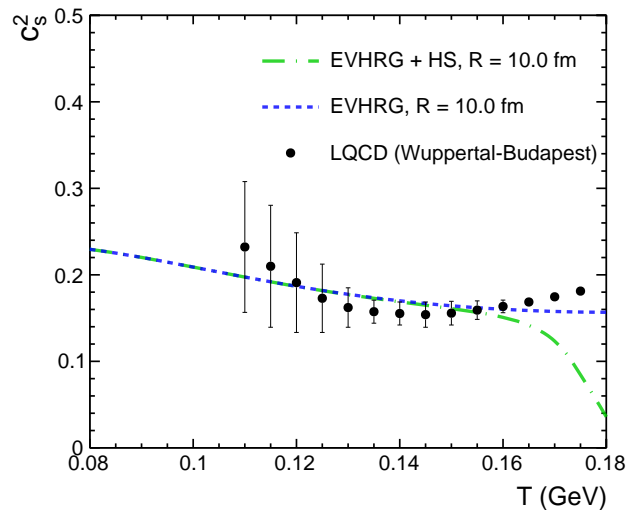


FIG. 2: The square of the speed of sound (c_s^2) as a function of temperature (T). This is compared with lattice data [38].

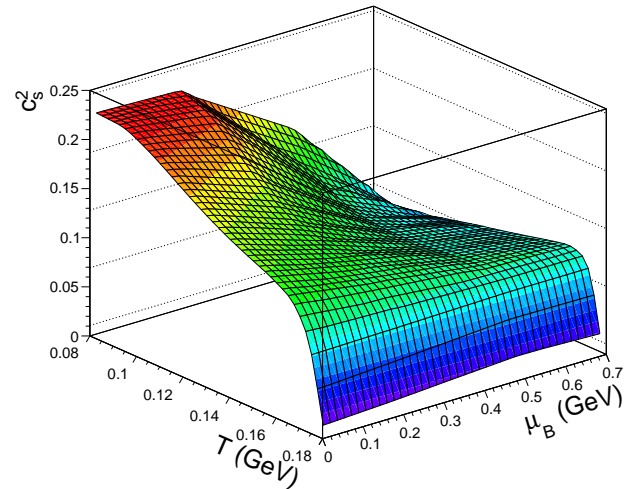


FIG. 3: The c_s^2 as a function of temperature and μ_B for $R = 10.0$ fm.

that increasing temperature at very low chemical potential ($\mu_B = 0 - 0.2$ GeV) gives the similar results as discussed in Fig. 2. However, at $\mu_B > 0.2$ GeV with increasing T speed of sound (or c_s^2) decreases initially up to $T \sim 0.140$ GeV and then start increasing with temperature. As μ_B increases the c_s^2 dip point on the T -axis shifts towards the lower temperature end. This smooth change in the behaviour of c_s^2 with high μ_B mimics the phase transition at $T < T_c \approx 0.160$ GeV. The sudden drop in the c_s^2 at high T is caused by the same effect of the Hagedorn states as seen in Fig. 2.

Reynolds number, Re , is an important parameter

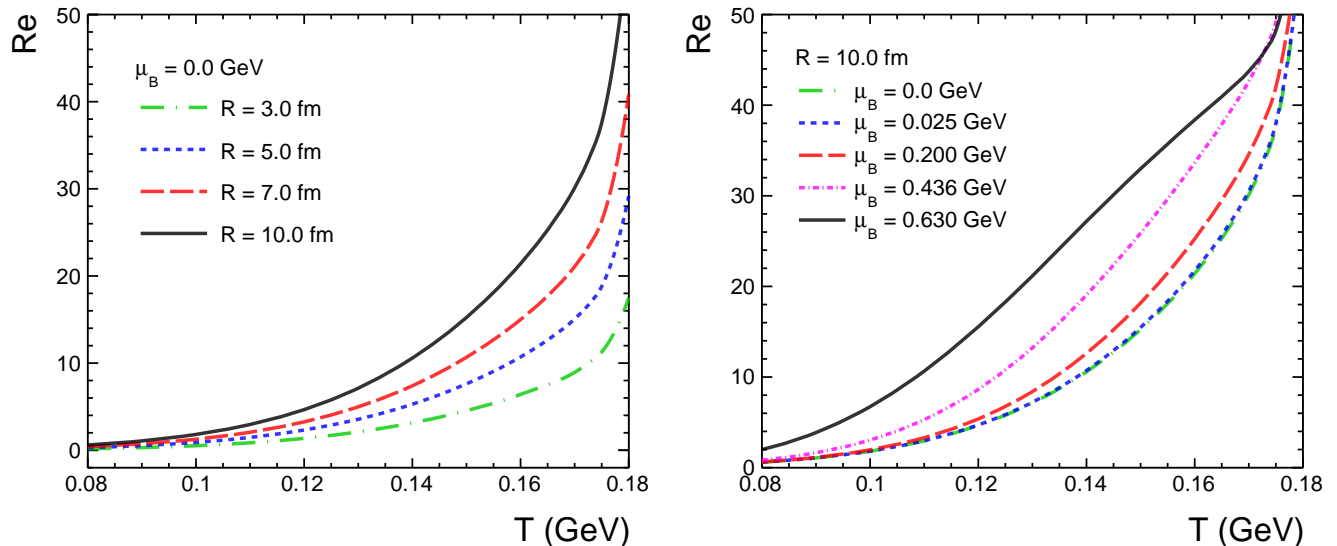


FIG. 4: Reynolds number as a function of temperature for different values of R at $\mu_B = 0$ GeV (left panel) and different values of μ_B at $R = 10.0$ fm, which is the case of heavy-ion collisions (right panel).

in hydrodynamics that contains information regarding instabilities in the fluid. A very high Reynolds number is usually associated with the turbulence in the fluid. The inverse of Reynolds number, Re^{-1} , is generally seen as a proxy for η/s in ultra-relativistic heavy-ion collisions as both of them are directly related. As a result of this relation, $Re \gg 1$ implies inviscid flow. We present the dependence of Reynolds number on system size in Fig. 4. We note that it increases with temperature for all values of R , indicating that the system becomes less viscous at higher temperatures and approaches a 'perfect fluid' limit. Fig. 4 also explores the variation of Reynolds number with chemical potential (right panel). We have chosen five different values of chemical potentials; $\mu_B = 0.0, 0.025, 0.200, 0.436$ and 0.630 GeV, which corresponds to LHC energies, RHIC at $\sqrt{s_{NN}} = 200$ GeV and $\sqrt{s_{NN}} = 19.6$ GeV, RHIC/FAIR at $\sqrt{s_{NN}} = 7.7$ GeV and NICA at $\sqrt{s_{NN}} = 3$ GeV respectively [39–42]. The system radius is fixed at 10.0 fm, which roughly corresponds to ultra-relativistic heavy-ion collisions. At low temperatures, Re increases with μ_B indicating that viscosity of the system decreases with increasing μ_B . As it appears, at higher temperature the Reynolds number, Re , becomes almost independent of the baryochemical potential of the system.

Large values for the Knudsen number, Kn , imply that the system is far from thermodynamic equilibrium, while small values, tending to zero, indicate a high degree of thermalization within the system. Fig. 5 shows the dependence of Knudsen number with system radius. We see a lower value of Kn even at low temperatures for large R . This indicates that larger systems have a higher tendency to achieve thermodynamic equilibrium. Kn is small at

high temperatures and does not vary much with system radius. This behavior is expected because at lower temperatures the mean free path (λ) is larger, indicating less interaction among the hadrons. The variation of Kn also indicates that the system formed at high temperatures is near to the equilibrium and therefore, we can apply hydrodynamics to study the evolution of the system. The variation of Knudsen number as a function of temperature for different chemical potentials is also shown in the right panel of Fig. 5. We see that Kn decreases with increase in μ_B .

Supersonic flows significantly impact two-particle correlations because of the formation of Mach cones. The interest in Mach cones formed in ultra-relativistic heavy-ion collisions was sparked from the two-particle correlations observed at RHIC [43, 44]. However, subsequent measurements at the LHC energies do not support these observations [45, 46]. It is argued that the structure observed might be an artifact of incorrect background considerations [47]. Although there is no direct experimental evidence for their existence, theoretical interest in Mach cones still persists as its disappearance could hint at a possible QCD critical point [48]. Mach number, Ma , being the ratio of characteristic flow velocity to the velocity of sound, could tell about the possible formation of Mach cones in the fluid. If $Ma \ll 1$, the density is almost uniform throughout the system and the fluid is incompressible. Fig. 6 depicts the variation of Mach number with system radius. We observe that Ma is independent of system radii at a particular temperature. As temperature increases, the system flow changes from subsonic to supersonic, indicating possible Mach cone formation.

It was observed that as η/s increases, the typical Mach

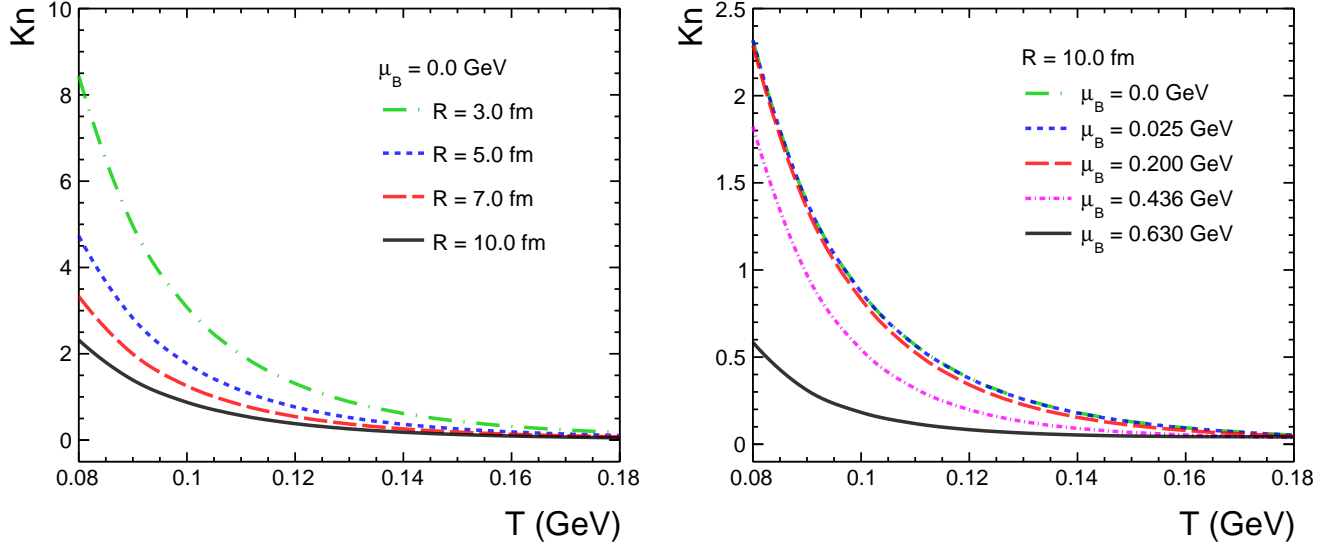


FIG. 5: Knudsen number, Kn , as a function of temperature for different values of system size, R at $\mu_B = 0.0$ GeV (left panel) and for different values of μ_B at $R = 10.0$ fm, which is the case of larger systems (right panel).

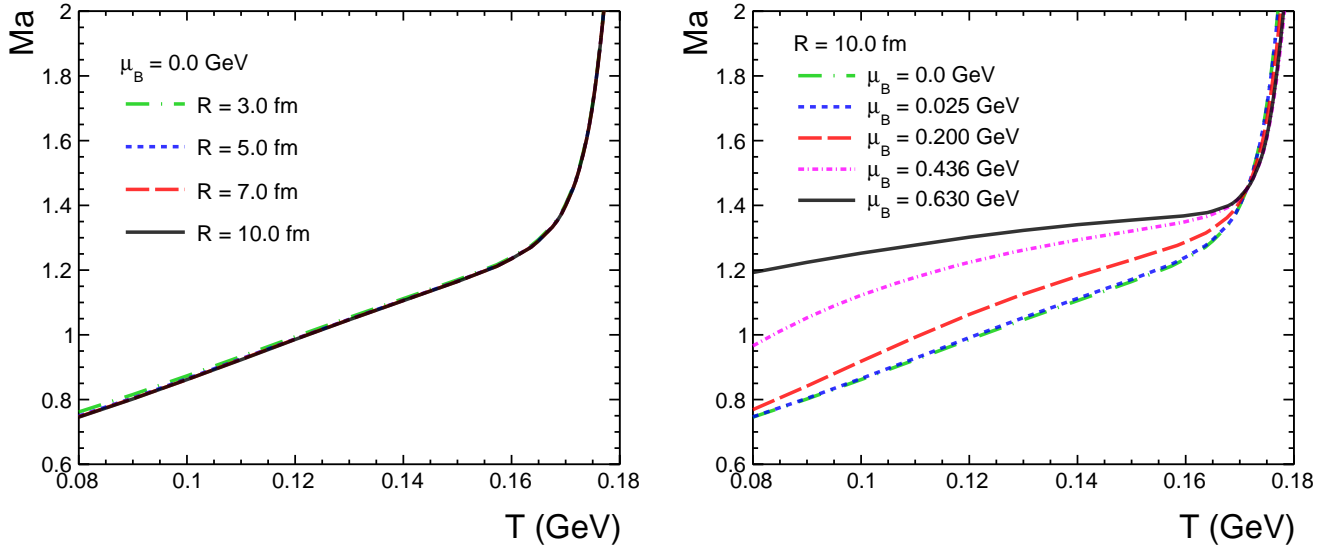


FIG. 6: Mach number, Ma , as a function of temperature for different values of system size, R at $\mu_B = 0.0$ GeV (left panel) and for different values of μ_B at $R = 10.0$ fm, for larger systems (right panel).

cone structure smears out and vanishes [49, 50]. Right panel of Fig. 6 suggests the dependence of Mach number on μ_B . We see that it increases with increasing μ_B and remains above the supersonic limit at all temperatures for the highest value of μ_B considered here. This might be an indication of the early formation of a rapidly expanding system with shock waves at higher μ_B values. From Fig. 6, it can also be inferred that since Mach number is of the order of unity for all temperatures and at all values of μ_B , the system produced in ultra-relativistic collisions is compressible [15].

IV. SUMMARY

In summary, we have estimated various relevant parameters like Reynolds number, Knudsen number and Mach number which assist in characterizing many-particle system. The dependence of these parameters on the system size, temperature, chemical potential for hadrons produced in ultra-relativistic nuclear collisions have been investigated. The obtained values ($Kn \ll 1$, $Ma \sim 1$ and $Re \gg 1$) indicate the occurrence of compressible inviscid flows at high temperatures close to the

phase transition region ($T \sim 150 - 170$ MeV). The degree of thermalization of hadron gas estimated is comparable over different system sizes, indicating the applicability of hydrodynamics in interpreting the results from high multiplicity pp to heavy-ion collisions. This puts into question the applicability of pp collisions as a baseline for heavy-ion collisions at the high beam energies presently accessible at different particle accelerators.

Acknowledgment

This research work has been carried out under financial supports from DAE-BRNS, the Government of India,

Project No. 58/14/29/2019-BRNS of Raghunath Sahoo. For the research fellowship, Ronald Scaria acknowledges CSIR, Govt. of India. CRS and RS acknowledge the financial supports under the above BRNS project. Further R.S. acknowledges the financial supports under the CERN Scientific Associateship, CERN, Geneva, Switzerland. The authors acknowledge the Tier-3 computing facility in the experimental high-energy physics laboratory of IIT Indore supported by the ALICE project.

-
- [1] P. Kovtun, D. T. Son and A. O. Starinets, Phys. Rev. Lett. **94**, 111601 (2005).
- [2] I. Arsene et al. (BRAHMS Collaboration), Nucl. Phys. A **757**, 1 (2005).
- [3] B. B. Back et al. (PHOBOS Collaboration), Nucl. Phys. A **757**, 28 (2005).
- [4] J. Adams et al. (STAR Collaboration), Nucl. Phys. A **757**, 102 (2005).
- [5] K. Adcox et al. (PHENIX Collaboration), Nucl. Phys. A **757**, 184 (2005).
- [6] J. Adam et al. (ALICE Collaboration), Nat. Phys. **13**, 535 (2017).
- [7] V. Khachatryan et al. (CMS Collaboration), Phys. Lett. B **765**, 193 (2017).
- [8] D. Velicanu [CMS Collaboration], J. Phys. G **38**, 124051 (2011).
- [9] R. Campanini and G. Ferri, Phys. Lett. B **703**, 237 (2011).
- [10] D. Thakur, S. De, R. Sahoo and S. Dansana, Phys. Rev. D **97**, 094002 (2018).
- [11] D. Sahu, S. Tripathy, R. Sahoo and S. K. Tiwari, [arXiv:2001.01252 [hep-ph]].
- [12] W. T. Deng and X. G. Huang, Phys. Rev. C **93**, 064907 (2016).
- [13] R. S. Bhalerao, J. P. Blaizot, N. Borghini and J. Y. Ollitrault, Phys. Lett. B **627**, 49 (2005).
- [14] H. J. Drescher, A. Dumitru, C. Gombeaud and J. Y. Ollitrault, Phys. Rev. C **76**, 024905 (2007).
- [15] J-Y Ollitrault, Eur. J. Phys. **29**, 275 (2008).
- [16] A. Andronic, P. Braun-Munzinger, J. Stachel, and M. Winn, Phys. Lett. B **718**, 80 (2012).
- [17] V. Vovchenko, D. V. Anchishkin, and M. I. Gorenstein, Phys. Rev. C **91**, 024905 (2015).
- [18] D. H. Rischke, M. I. Gorenstein, H. Stöcker, W. Greiner, Z. Phys. C **51**, 485 (1991).
- [19] R. Hagedorn and J. Ranft, Nuovo Cim. Suppl. **6**, 169 (1968).
- [20] G. P. Kadam and H. Mishra, Phys. Rev. C **92**, 035203 (2015).
- [21] Mirco Cannoni, Phys. Rev. D **89**, 103533 (2014).
- [22] P. Gondolo and G. Gelmini, Nucl. Phys. B **360**, 145 (1991).
- [23] S. K. Tiwari, S. Tripathy, R. Sahoo and N. Kakati, Eur. Phys. J. C **78**, 938 (2018).
- [24] G. Kadam and S. Pawar, Adv. High Energy Phys. **2019**, 6795041 (2019).
- [25] J. Noronha-Hostler, J. Noronha, and C. Greiner, Phys. Rev. C **86**, 024913 (2012).
- [26] J. Noronha-Hostler, J. Noronha, and C. Greiner, Phys. Rev. Lett. **103**, 172302 (2009).
- [27] P.A. Zyla et al. (Particle Data Group), PTEP **2020**, no.8, 083C01 (2020).
- [28] P. Braun-Munzinger, I. Heppe, J. Stachel, Phys. Lett. B **465**, 15 (1999).
- [29] K. Redlich and K. Zalewski, arXiv:1611.3746 (2016).
- [30] A. Bhattacharyya, R. Ray, S. Samanta and S. Sur, Phys. Rev. C **91**, 041901(R) (2015).
- [31] N. Sarkar and P. Ghosh, Phys. Rev. C **96**, 044901 (2017).
- [32] S. Chatterjee, S. Das, L. Kumar, D. Mishra, B. Mohanty, R. Sahoo and N. Sharma, Adv. High Energy Phys. **2015**, 349013 (2015).
- [33] D. Sahu, S. Tripathy, G. S. Pradhan and R. Sahoo, Phys. Rev. C **101**, 014902 (2020).
- [34] S. Acharya *et al.* [ALICE], Phys. Lett. B **802**, 135225 (2020).
- [35] M. Gorenstein, M. Hauer, O. Moroz, Phys.Rev.C **77**, 024911 (2008).
- [36] G.S. Denicol, C. Gale, S. Jeon, and J. Noronha, Phys. Rev. C **88**, 064901 (2013).
- [37] G. Kadam and H. Mishra, Phys. Rev. D **100**, 074015 (2019).
- [38] S. Borsányi, Z. Fodor, C. Hoelbling, S. D. Katz, S. Krieg, K. K. Szabó, Phys. Lett. B **730**, 99 (2014).
- [39] N. A. Tawfik, L. I. Abou-Salem, A. G. Shalaby, M. Hanafy, A. Sorin, O. Rogachevsky and W. Scheinast, Eur. Phys. J. A **52**, 324 (2016).
- [40] P. Braun-Munzinger, D. Magestro, K. Redlich and J. Stachel, Phys. Lett. B **518**, 41 (2001).
- [41] J. Cleymans, H. Oeschler, K. Redlich and S. Wheaton, Phys. Rev. C **73**, 034905 (2006).
- [42] A. Khuntia, S. K. Tiwari, P. Sharma, R. Sahoo and T. K. Nayak, Phys. Rev. C **100**, 014910 (2019).
- [43] M. M. Aggarwal et al. (STAR collaboration), Phys. Rev. C **82**, 024912 (2010).
- [44] A. Adare et al. (PHENIX collaboration), Phys. Rev. Lett. **104**, 252301 (2010).
- [45] G. Aad et al. (ATLAS collaboration), Phys. Lett. B. **739**, 320 (2014).

- [46] S. Chatrchyan et al. (CMS collaboration), Phys. Rev. C. **90**, 024908 (2014).
- [47] C. Nattrass, N. Sharma, J. Mazer, M. Stuart and A. Bejnood, Phys. Rev. C. **94**, 011901 (2016).
- [48] G. Sarwar, M. Hasanujjaman, M. Rahaman, A. Bhat-tacharyya and Jan-e Alam, Phys. Lett. B **820**, 136583 (2021).
- [49] I. Bouras, A. El, O. Fochler, H. Niemi, Z. Xu, C. Greiner, Phys. Lett. B **728**, 156 (2014).
- [50] I Bouras et al, J. Phys.: Conf. Ser. **270**, 012012 (2011).